International Journal of Thermal Sciences 100 (2016) 448–456

Contents lists available at ScienceDirect

International Journal of Thermal Sciences

journal homepage: www.elsevier.com/locate/ijts

Numerical studies on thermo-hydraulic characteristics of laminar flow in a heat exchanger tube fitted with vortex rods

Nianben Zheng, Peng Liu, Feng Shan, Jiaju Liu, Zhichun Liu, Wei Liu*

School of Energy and Power Engineering, Huazhong University of Science and Technology, Wuhan 430074, China

ARTICLE INFO

Article history:
Received 22 January 2015
Received in revised form
5 September 2015
Accepted 5 September 2015
Available online 14 October 2015

Keywords:
Vortex rods
Longitudinal swirling flow
Heat transfer enhancement
Pressure drop
Laminar flow

ABSTRACT

An analysis of the thermo-hydraulic characteristics of a heat exchanger tube fitted with a novel vortex rod insert has been conducted numerically under uniform heat flux conditions. The vortex rods had three relative rod length ratios ($LR = b/D = 0.15$, 0.25, and 0.35) and three relative rod pitch ratios ($PR = p/D = 1$, 1.5, and 2), and they were studied for numerous Reynolds numbers (Re) that ranged from 300 to 1800 using water as the working fluid. With these vortex rods, longitudinal swirling (or vortex) flow can be generated for better fluid mixing between the wall and core flow regions, thereby allowing for a high heat transfer rate with a moderate increase in the pressure drop. The results indicate that the presence of the vortex rods elicits a considerable heat transfer enhancement in the tube, $Nu/Nu_0 = 1.1–3.9$, with an increase in pressure drop, and $f/f_0 = 1.4–5.3$. Both the Nu/Nu_0 and the f/f_0 ratios increase with Re and LR increases and with PR decreases. The performance evaluation criterion (PEC) values of all vortex rod cases are above unity except for the cases with $LR = 0.15$ at $Re = 300$. The case at which $LR = 0.35$ and $PR = 1$ provides the maximum PEC value of approximately 2.22 at $Re = 1800$. These results provide evidence that the vortex rod insert is a promising technique for laminar convection heat transfer enhancement.

1. Introduction

Heat exchangers are extensively used in many engineering areas, such as air-conditioning, power generation, the chemical processing, waste heat recovery, and steel production. In order to improve the heat transfer rate and the thermal performance, and reduce the size of the heat transfer system, thereby reducing installation and operating costs, heat transfer enhancement techniques are usually needed [1]. These techniques can be classified into two group types. The first refers to active methods that require extra external power sources. The other refers to the passive method that requires no extra external power sources for the systems [2]. In general, the passive method is more frequently applied in practical situations and has drawn significant attention because of its rapid installation, easy maintenance, and low cost. One important group relevant to the passive method type includes inserted elements, such as helical or twisted tapes, coil wires, vortex rings, louvered strips, and angled fins. These elements typically function as vortex or swirl generators by generating longitudinal swirling flow and modifying the velocity distribution. This induces a better fluid mixing between the central region and the region close to the wall and thus enhances the heat transfer rate. However, this technique is realized at the cost of an increase in the pressure drop. It is challenging to achieve an enhancement in the heat transfer rate with a moderate flow resistance.

Motivated by the realization of an object that achieves a high heat transfer rate without much increase in the pressure drop, researchers all over the world have expended tremendous efforts towards the investigation of various insert elements. Since Whitham [3] reported that the twisted tape could improve heat transfer in heat exchangers, the utilization of twisted tapes for heat transfer enhancement has been extensively reported. Saha et al. [4] experimentally investigated the heat transfer under laminar flow conditions and the pressure drop characteristics in a circular tube fitted with regularly spaced twisted tape elements connected by thin circular rods. In their study, they found that regularly spaced twisted tape performed significantly better than the full-length twisted tape at high Reynolds numbers, and that the pressure drop decreased by 40%. Wang et al. [5] presented the configuration optimization of a regularly spaced short-length twisted tape in a circular tube for turbulent heat transfer using computational fluid dynamics (CFD) modeling. Delta-winglet twisted tape inserts were

* Corresponding author. Tel.: +86 27 87542618; fax: +86 27 87540724.
E-mail address: w_liu@hust.edu.cn (W. Liu).

http://dx.doi.org/10.1016/j.ijthermalsci.2015.09.008
1290-0729/

experimentally investigated by Eiamsa-ard and his co-workers [6]. The elicited results show that the mean Nusselt number and the mean friction factor increased with a decreasing twisted ratio and an increasing depth of the wing-cut ratio. Subsequently, Eiamsa-ard and Promvonge [7] assessed the performance of alternate clockwise and counterclockwise twisted tape inserts used in a heat exchanger tube. Recently, Eiamsa-ard and Kiatkittipong [8] studied the thermal performance effects of multiple twisted tapes placed in different arrangements, using TiO_2 nanoparticles (at different concentrations) as the working fluid. By conducting a numerical study on the heat transfer and friction characteristics of laminar flow in a tube fitted with center-cleared twisted tape, Guo et al. [9] demonstrated that the flow resistance could be reduced using narrow width and center-cleared twisted tapes. Zhang et al. [10] presented a simulation of multi-longitudinal vortices induced in a tube by triple and quadruple twisted tapes. Helical screw tape is a modified form of a twisted tape. Unlike the twisted tape that generates swirling flow in two parallel flow directions, helical screw tape, provides a single, smooth, helical direction of flow that reduces the pressure drop significantly. Zhang et al. [11] performed a physical quantity synergy analysis to investigate the mechanism of the heat transfer enhancement of a tube fitted with helical screw tape without core rod inserts, and conducted an entropy generation analysis to optimize the helical screw tape. Helical wire coils fitted inside a round tube were experimentally studied by Garcia [12] to characterize the thermo-hydraulic behavior in laminar, transient, and turbulent flows. Saraç and Bali [13] carried out a study on heat transfer and pressure drop characteristics of a decaying swirling flow produced by the insertion of vortex generators with a propeller geometry. An experimental investigation on turbulent convection in a round tube equipped with propeller-type swirl generators was undertaken by Eiamsa-ard et al. [14]. Their results indicate that the use of the propeller led to a maximum efficiency enhancement of 1.2. Naphon [15] studied the heat transfer characteristics and pressure drop of the coil wire insert that could enhance the heat transfer significantly, especially in the laminar region. Yakut et al. [16,17] reported the effects of conical ring turbulators on heat transfer, pressure drop, flow-induced vibration, and vortices, based on the evaluation of entropy generation, revealing that the conical ring turbulators show merits as energy-saving devices only at low Reynolds numbers, since a low pressure drop is generated in the flow region. Promvonge and Eiamsa-ard [18] experimentally examined the combined effects of the conical ring and twisted tape in a circular tube. The conical strip insert is a modification of the conical ring. Guo et al. [19] studied the thermo-hydraulic performance of a conical strip for reducing the upwind area, and found that the performance factor could be enhanced by 36–61% if conical ring inserts were replaced with conical strip inserts for turbulent flows within a *Re* range of 5000–25,000. Fan et al. [20] numerically investigated the heat transfer and flow characteristics of a circular tube inserted with louvered strips. Their results demonstrate that the louvered strip is a promising tube insert that could be extensively used for heat transfer enhancement of turbulent flows.

Recently, some new types of inserts have been developed [21–24]. Caliskan [21] performed an experimental investigation of heat transfer in a channel with new winglet-type vortex generators using the infrared thermal imaging technique. A nonconventional insert fabricated with a central rod on which curved delta-wing vortex generators were attached on opposite sides (at specific axial locations) was presented by Deshmukh and Vedula [22]. Promvonge et al. [23] introduced and used a novel inclined vortex ring turbulator for heat transfer enhancement that aimed to create counter-rotating vortices inside the tube to help increase the turbulence intensity, and to convey the colder fluid from the core region to the heated wall region. Tu et al. [24] experimentally investigated the characteristics of heat transfer and the friction factor in turbulent flow through a circular tube with small pipe inserts. Their results show that pipe inserts could transfer more heat for the same pumping power given for their unique structure, compared to other inserts.

Based on the literature publications listed above, the use of conventional inserts, such as the twisted tape, helical screw tape, and the propeller-type swirl generator, will inevitably result in a large increase in the friction factor (even though the heat transfer can also be increased at the same time), thus leading to a low thermo-hydraulic performance. The new types of inserts utilized in Refs. [21–24] are considerably simple in structure compared to conventional inserts. Moreover, they can still function as vortex or swirl generators for mixing fluids by conveying the colder fluid from the core region to that of the heated-wall region, and result in uniformity of temperature with moderate flow resistance. In addition, Liu and his co-workers [25–27] pointed out that longitudinal swirling flow with single vortex or multi-vortexes could lead to heat transfer enhancement without much increase in the pressure drop, from the viewpoint of heat transfer optimization. These prior research studies have provided the authors a hint, in that, it is possible to design a simple structure to generate longitudinal swirling flow to mix fluids. In this work, a novel insert element has been proposed, called “vortex rods,” consisting of thin rods. Vortex rods act as vortex generators. The geometries of vortex rod inserts are shown in Fig. 1, where some thin rods are mounted on three straight rods and are inserted in the tube. The utilization of the vortex rod inserts is expected to achieve a high heat transfer rate with moderate pressure drop owing to the longitudinal swirling flow generated by the vortex rod inserts. In the present study, a numerical analysis of the thermo-hydraulic characteristics

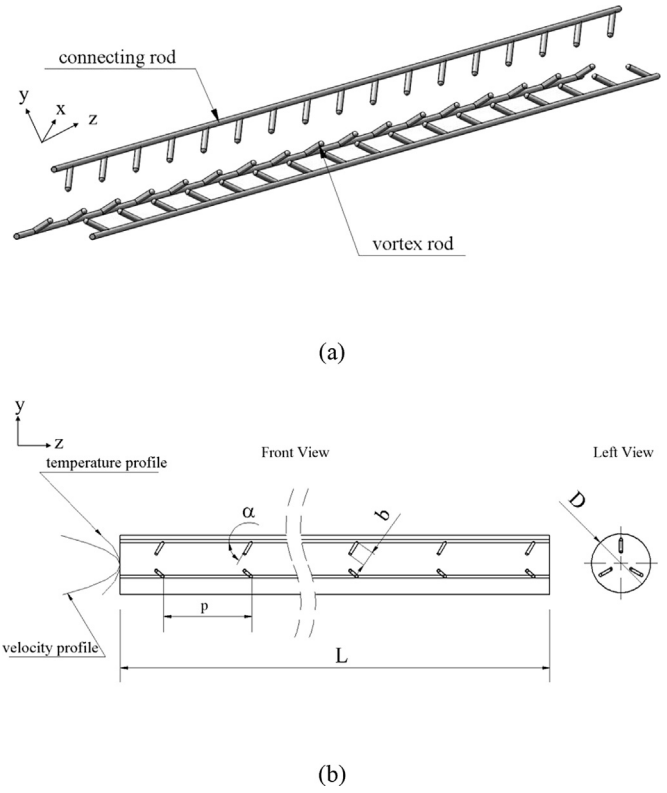

Fig. 1. Schematic diagram of (a) the vortex rods and (b) a tube fitted with vortex rods.

is presented in a heat exchanger tube fitted with vortex rods under laminar flow conditions, using water as the working fluid.

2. Physical model

The geometries of the vortex rods are depicted in Fig. 1. Vortex rods made of stainless steel (0.001 m in diameter) are mounted on three connecting rods of 0.001 m in diameter and are inserted in the tube. The slant angle (α) of the vortex rods is fixed at 60°. The length (L) and diameter (D) of the tube are 0.5 m and 0.02 m, respectively. The length and pitch of the vortex rods are denoted as b and p, respectively. The effects of three relative rod length ratios ($LR = b/D = 0.15$, 0.25, and 0.35) and three relative rod pitch ratios ($PR = p/D = 1$, 1.5, and 2) on the thermo-hydraulic characteristics will be investigated.

3. Mathematical model and numerical methods

3.1. Governing equations and boundary conditions

The present problem under consideration is assumed to be three-dimensional, laminar, and steady. The following assumptions are made for the derivation of the governing equations: (1) the vortex rods are stiff and thus the vibration and deformation are neglected, (2) the fluid is continuous and incompressible, and (3) the influences of gravity and viscous heating are not taken into consideration. Equations of continuity (Eq. (1)), momentum (Eq. (2)), and energy (Eq. (3)), for the fluid flow are given in a tensor form, as listed below. In particular,

$$\frac{\partial(\rho u_i)}{\partial x_i} = 0 \tag{1}$$

$$\frac{\partial}{\partial x_j}(\rho u_i u_j) = -\frac{\partial P}{\partial x_i} + \frac{\partial}{\partial x_j}\left[\mu\left(\frac{\partial u_i}{\partial x_j} + \frac{\partial u_j}{\partial x_i}\right)\right] \tag{2}$$

where ρ is the density of fluid, u_i is a mean component of velocity in the direction of x_i, P is the pressure, and μ is the dynamic viscosity of water.

$$\frac{\partial}{\partial x_j}\left(\rho u_j C_p T - k\frac{\partial T}{\partial x_j}\right) = 0 \tag{3}$$

in which C_P and k are the specific heat at constant pressure and the thermal conductivity of the fluid, respectively.

To eliminate the inlet effect and guarantee a fully developed flow, the fully developed profiles of velocity and temperature are specified at the inlet [28], as indicated by Eqs. (4) and (5), respectively. At the outlet, a pressure-outlet condition is used. On the tube wall, a constant heat flux is imposed. No slip conditions are applied on the surfaces of the vortex rods and the tube wall.

$$u = u_c\left(1 - \frac{r^2}{R^2}\right) \tag{4}$$

$$T = T_c + \frac{qR}{k}\left[\left(\frac{r}{R}\right)^2 - \frac{1}{4}\left(\frac{r}{R}\right)^4\right] \tag{5}$$

where u_c and T_c are the velocity and temperature at the centerline of the tube, respectively. Moreover, q is the heat flux density on the tube wall, R is the inner radius of the tube, and r is the radial distance.

3.2. Simulation parameters

The Reynolds number (Re) is given by

$$Re = \frac{\rho u_m D}{\mu} \tag{6}$$

where u_m is the mean streamwise velocity in the tube.

The average heat transfer coefficient (h) and the Nusselt number (Nu) are estimated as follows:

$$h = \frac{q}{T_w - T_m} \tag{7}$$

$$Nu = \frac{hD}{k} \tag{8}$$

where T_w is the average temperature of the wall and T_m is the bulk temperature of the fluid.

Correspondingly, the friction factor (f) can be written as

$$f = \frac{\Delta P}{(L/D)\rho u_m^2/2} \tag{9}$$

in which ΔP could be determined by the difference between the mass-averaged pressures at the inlet and the outlet of the investigated region.

To evaluate the overall thermo-hydraulic performance of the enhanced tube at an identical pump power, the extensively used performance evaluation criterion (PEC) proposed by Webb [29] is adopted. It is calculated based on the following formula:

$$PEC = \frac{Nu/Nu_0}{(f/f_0)^{1/3}} \tag{10}$$

where Nu_0 and f_0 are the Nusselt number and the friction factor of the plain tube, respectively.

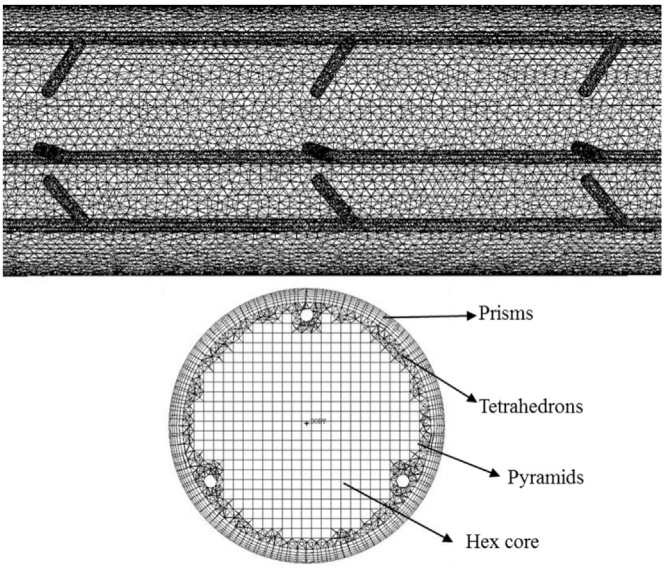

Fig. 2. Generation of meshes of the computation domain.

3.3. Grid system

The computational domain is resolved using an unstructured mesh generated with the commercial software ICEM CFD 14.0. The meshes consist of prisms, tetrahedrons, hex core, and pyramids, as shown in Fig. 2. To better simulate boundary layer effects, prism grids, which are orthogonal to the surfaces and with faces perpendicular to the boundary layer flow direction, are extruded from the surface of the tube. A Hex core mesh, with hexahedron grids filling the majority of the volume, is generated to capture the characteristics of the fluid flow in the core region. To fill the areas between the surface of the prisms and the hex core, tetrahedron grids are used. Pyramids are applied to establish a conformal connection between triangle and quadrangle faces. In addition, the local grid refinement is applied in the vicinity of the vortex and the connecting rods. Adaptive grid refinement is also performed during the preliminary computations. Grid independent tests of three different grid numbers (1771057, 2318640, and 3259193) for vortex rods with $LR = 0.25$ and $PR = 1.5$, at $Re = 1500$, have been conducted for validating the accuracy of numerical solutions. The Nu and f values obtained by the three grid systems are illustrated in Fig. 3. The results indicate that the deviation between the calculated values for the grids comprising 2318640 and 3259193 elements is considerably small. This finding demonstrates that the grid system with 2318640 elements is adequately dense for the simulations. Therefore, this grid system is adopted in the subsequent simulation reflecting a compromise of computational time and solution precision.

3.4. Numerical method

The commercial software Fluent 14.0 is used for the CFD simulations. The governing conservation equations accompanied by the boundary conditions are discretized using the finite volume formulation. The standard pressure and second order upwind discretization schemes for the momentum and energy equations are employed in the numerical model. To achieve pressure–velocity coupling, the semi implicit method for pressure-linked equations (SIMPLE) algorithm is selected because it is more stable and economical compared to other algorithms. The computation is assumed to be converged when the relative residual values are less than 10^{-6} for all variables and less than 10^{-8} for the energy equation, or when all the relative residual values are kept unchanged.

4. Results and discussion

4.1. Verification of smooth tube

The current numerical results are first validated in terms of the Nusselt number and the friction factor. The calculated Nusselt number and friction from the smooth tube case are compared to those of the well-known theoretical formulas, i.e., to 4.36 and 64/Re, respectively. Fig. 4 shows that the agreement between the computational results and the theoretical values is satisfactory (the relative discrepancy is within 6%), which demonstrates that the present numerical predictions have a reasonable accuracy.

4.2. Flow structures

Prior to discussing the results, it is necessary to understand the flow structure and behavior of the tube fitted with vortex rods. An effective method to visualize the flow in the tube inserted with vortex rods is to analyze the generated streamlines. These streamlines can then be used to capture the swirling motion associated with the vortices in the tube flow, as depicted in Fig. 5. The streamlines are presented for $Re = 900$ at $LR = 0.25$ and $PR = 1$. Fig. 5(a) and (b) shows the streamlines in transverse planes along the tube fitted with vortex rods and the streamlines in the streamwise direction with superimposed velocity maps, respectively. Fig. 6 presents the swirling strength iso-surface and the vortex core region. The effects induced by the vortex rods are represented by the mainstream flow separation and the vortex formation. As the incoming flow passes over the vortex rods, it separates into a multistream flow because of the pressure difference across the vortex rods before their helical motion along the tube.

From Fig. 5(a), it is observed that three pairs of counter-rotating vortices or longitudinal swirling flows are generated inside the tube. Each pair of longitudinal swirling flows is created by the rods mounted on the same connecting rod, and the mainstream flow is finally divided into six helical streams. To better visualize the coherent structure of the vortex, the streamlines along the streamwise direction with superimposed velocity maps are depicted in Fig. 5(b). Six helical streams are generated and evenly distributed along the tube. The direction and region of the vortex core can be visualized by considering the iso-surfaces of the swirling strength, as shown in Fig. 6. When the incoming flow

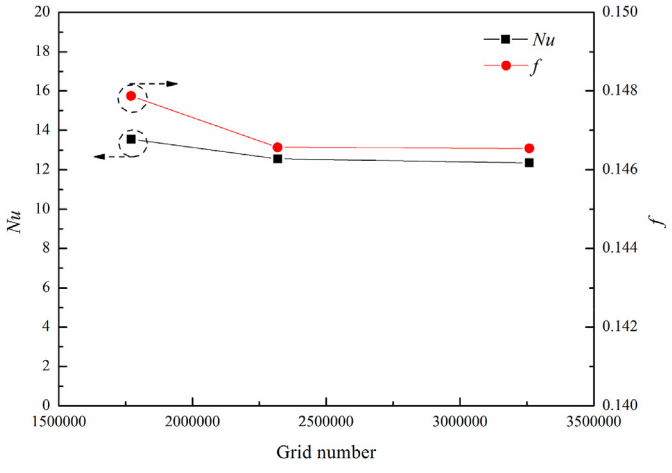

Fig. 3. Nusselt number and friction factor calculated by different grid systems for vortex rods with $LR = 0.25$ and $PR = 1.5$ at $Re = 1500$.

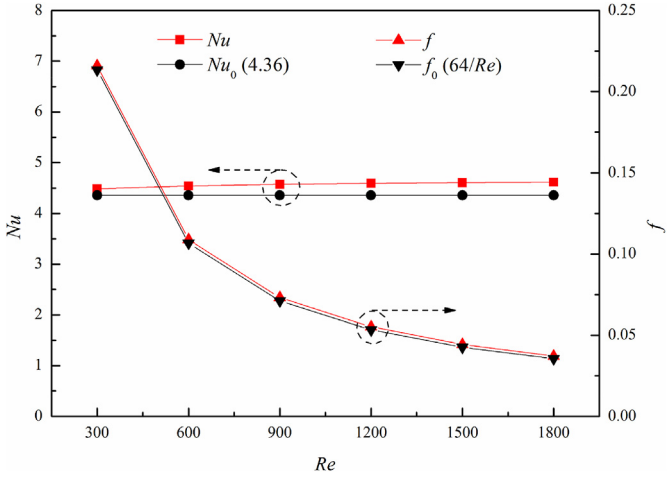

Fig. 4. Verification results for the Nusselt number and the friction factor for a smooth tube.

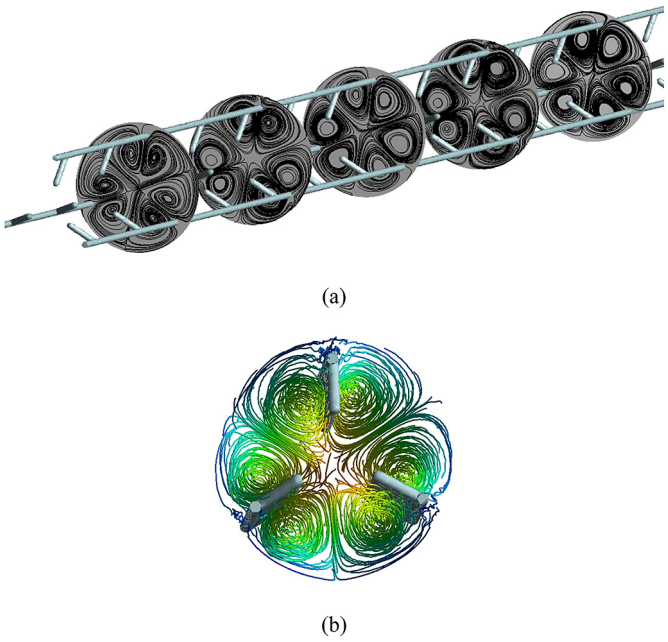

Fig. 5. Streamlines in (a) the transverse planes and (b) in the streamwise direction with superimposed velocity maps at $Re = 900$, $LR = 0.25$, and $PR = 1.5$.

passes over the vortex rods, three pairs of vortex cores (or equivalently, six vortex cores) are created behind the rods. The region of the vortex cores is small at first and increases gradually along the tube. This means that the swirling strength of the flow is gradually enhanced as the longitudinal swirling flow moves inside the tube. It can be concluded that the flow structure of the tube fitted with vortex rods is considerably different from that of the smooth tube. The flow pattern in the presence of the vortex rods results in a long flow path and relatively intense flow mixing between the wall and the core flow regions.

4.3. Heat transfer

Fig. 7 shows the temperature distribution on the wall of the tube fitted with vortex rods under a uniform heat flux condition. There is a major change in the temperature distribution on the tube wall. The temperature of the tube wall is high on some parts and low on other parts, indicating that the longitudinal swirling flow induced by the vortex rods influences significantly the temperature field since it can induce better fluid mixing between the wall and the core flow regions.

The 3-D plot of local Nusselt number on the tube wall along the flow direction is displayed in Fig. 8. The local Nusselt number was calculated by:

$$h_{local} = \frac{q}{T_{local} - T_m} \tag{11}$$

$$Nu_{local} = \frac{h_{local} D}{k} \tag{12}$$

where h_{local} is the local heat transfer coefficient, T_{local} is the local wall temperature.

It is evident from Fig. 8 that there is a major change in the local Nusselt number distribution on the tube wall. The area near the vortex robs has relatively higher Nusselt number. This can be attributed to the longitudinal swirling flow induced by the vortex rod that fluids between the wall and core flow regions are better mixed, and more heat is conveyed from the wall.

To reveal the major change in the temperature distribution, a closer inspection of the temperature field in the transverse plane of $z^* = z/L = 0.5$ and at $Re = 900$ with superimposed velocity vectors has been conducted, as depicted in Fig. 9. In the figure, it is apparent that three pairs of counter-rotating vortices near the wall are generated behind the vortex rods. The interaction between the counter-rotating vortices induced by each vortex rod generates an impingement zone near the wall. Thus, three impingement zones (denoted as A1, A2, and A3) are created. In these zones, cold fluids are swallowed from the core flow region and then impinged on the tube wall resulting in a high temperature gradient and a thin boundary layer near the wall. The high momentum of the fluid on the wall directly enhances the heat transfer from the impinged surface. Therefore, the temperature values in these zones are higher than those in the core region but relatively lower than those in other zones.

The interaction between the adjacent vortices created by different rods also induces three impingements zones (denoted as B1, B2, and B3). The direction of these impingements is towards the core flow region that is different from that of the impingements created by counter-rotating vortices. A distinctive feature in B1, B2, and B3, especially in the regions near the tube wall, is the impingement of some parts of the two vortices flowing in opposite directions. As a result of the impingement, the velocity of fluids in the transverse plane is much reduced and the swirling strength of the vortex flow is weakened at the same time, leading to the relatively low temperature gradient near the wall. In other words, the heat transfer rate in the regions near the tube wall is reduced, and this explains why the temperature values in these regions are higher than those in other zones. Except for the parts flowing in opposite directions, two vortices flow together and impinge

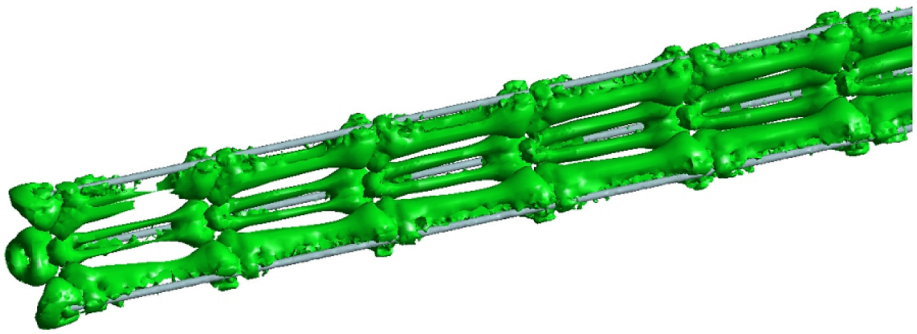

Fig. 6. Vortex core region at $Re = 900$, $LR = 0.25$, and $PR = 1.5$.

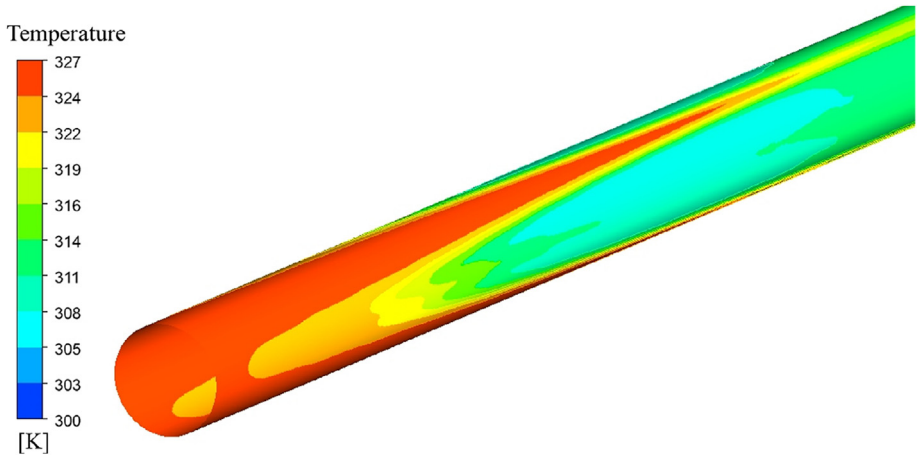

Fig. 7. Temperature distribution on the wall of the tube fitted with vortex rods.

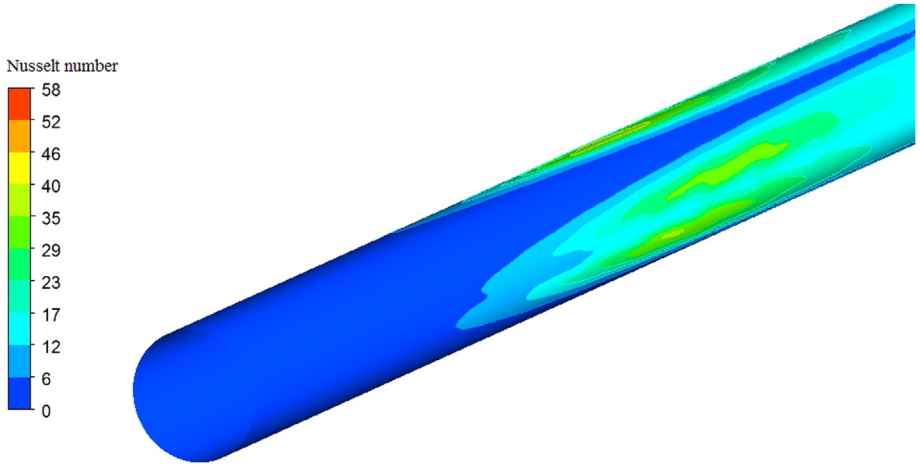

Fig. 8. 3-D plot of local Nusselt number on the tube wall along the flow direction.

towards the core flow region. This leads to a better fluid mixing between the wall and the core flow regions. In conclusion, the interaction between the vortex flows results in seven zones (six zones near the tube wall and one zone in the middle of the tube), covering almost the entire cross-sectional area, and reflected by a chaotic fluid mixing pattern within the tube except for the three small regions near the wall. The phenomena described above lead to an excellent heat transfer pattern indicated by a thin thermal boundary layer and the high temperature gradient.

Fig. 10 shows the contour plots of the temperature field in transverse planes ($z^* = 0.3$, 0.5, 0.7, and 0.9) along the tube for vortex rods with $LR = 0.15$, 0.25, and 0.35, at $Re = 900$ and $PR = 1$. The temperature fields at different transverse planes are similar for the same LR values. The only differences exist in the regions of these

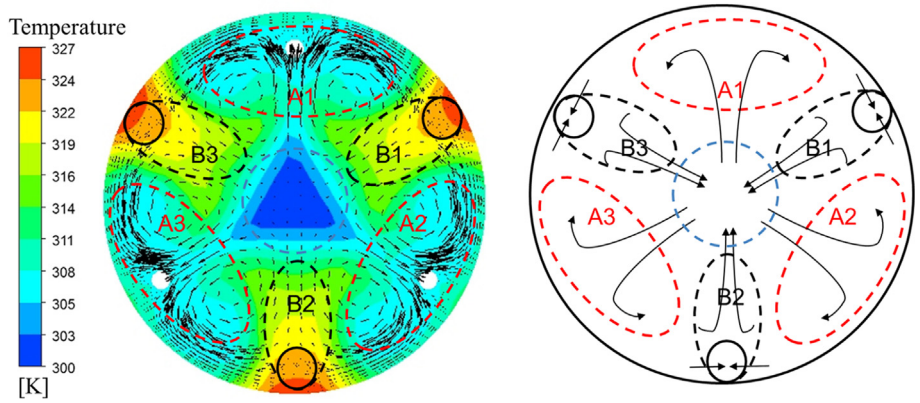

Fig. 9. Temperature distribution in the transverse plane at $z^* = 0.5$ and at $Re = 900$.

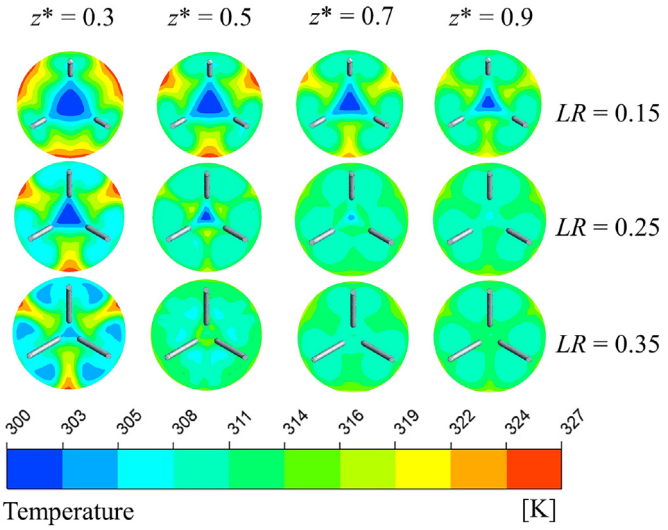

Fig. 10. Contour plots of the temperature field in transverse planes with $LR = 0.15$, 0.25, and 0.35, at $Re = 900$ and $PR = 1$.

fields where higher and lower (than average) temperatures are recorded. Because of the excellent fluid mixing between the wall and the core regions, the regions where higher and lower temperature values are noted are reduced gradually in space, and temperature fields are distributed almost uniformly within the entire flow. It is noted that there is a major change in the temperature distributions for different LR values within the same transverse plane. The temperature field distributes more uniformly with an increase in LR values since larger LR values imply the existence of longer vortex rods. Therefore, the range of the disturbance induced by the vortex rods is expanded. More cold fluids impinge towards the wall and hot fluids towards the core region, thereby indicating the merits of employing longer vortex rods for enhanced heat transfer.

Fig. 11 shows the temperature distributions in various transverse planes with $PR = 1, 1.5, 2$, at $Re = 900$ and $LR = 0.15$, reflecting the development of the temperature field along the tube fitted with vortex rods. All three cases studied demonstrate the similar developing trend, namely, that the uniformity of the temperature field increases gradually along the tube owing to the longitudinal swirling or vortex flow pattern induced by the vortex rods. The fluids between the wall and the core regions are better mixed at lower PR values. This is because more vortex rods are inserted in the tube (with a fixed length) at a lower pitch ratio, so the strength of the longitudinal swirling flow is enhanced.

The variation of the Nu/Nu_0 ratio with Re for vortex rods at various LR and PR values is shown in Fig. 12. The Nu/Nu_0 ratio tends to increase with the rise of Re and LR values for all PR values. A higher PR value leads to a decrease in the value of Nu/Nu_0. Vortex rods with $LR = 0.35$ and $PR = 1$ elicit the highest Nu/Nu_0 value. The maximum Nu/Nu_0 at $LR = 0.35$ is found to be approximately 3.9 for $PR = 1$, and approximately 3.6 and 3.2 for $PR = 1.5$ and $PR = 2$ respectively. A better assessment of the results plotted in Fig. 12 reveals that the use of the vortex rods at the different LR and PR values studied yields heat transfer rates of approximately 1.1–3.9 times higher compared to the smooth tube with no vortex rods, depending on the choice of the LR and PR values. The heat transfer enhancement indicated by the thin thermal boundary layer and the high temperature gradient can be attributed to the longitudinal swirling flow induced by the vortex rods.

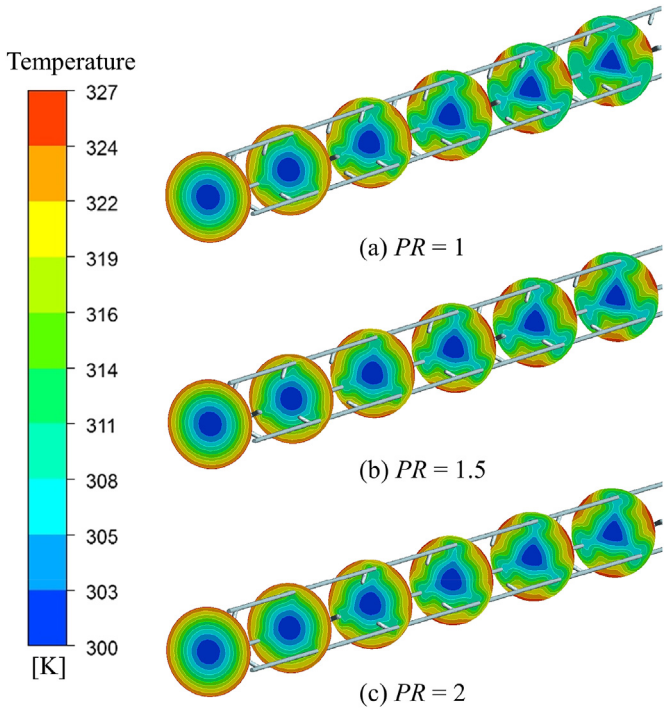

Fig. 11. Temperature distributions in transverse planes with $PR = 1, 1.5, 2$, at $Re = 900$ and $LR = 0.15$.

4.4. Pressure drop

Fig. 13 shows the variation of the friction factor ratio f/f_0 with Re values for vortex rods at various LR and PR values. According to the figure, the friction factor ratio is found to increase with increases in Re and LR values but to decrease with increasing PR values. The $PR = 1$ vortex rod case provides the highest f/f_0 value, while the $PR = 2$ vortex rod case yields the lowest f/f_0 value for all LR values. The friction factor for the vortex rods is approximately 1.4–5.3 times higher than that of the smooth tube. The pressure loss in terms of the friction factor for the tube fitted with vortex rods can be explained by the dissipation of the dynamic pressure of the fluids caused by the combined effect of the flow blockage (due to

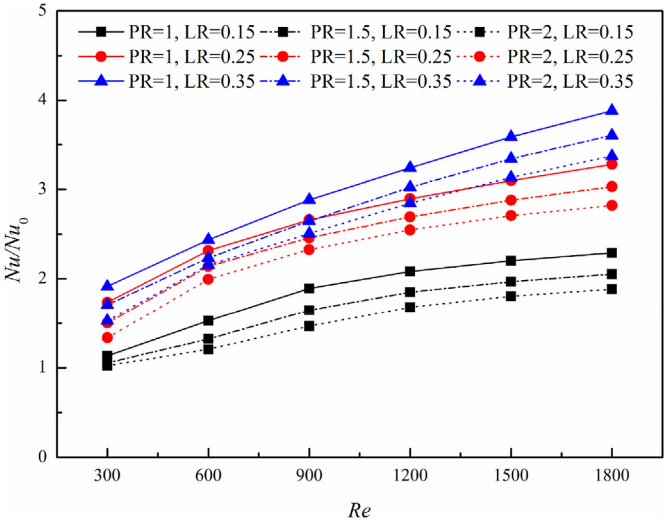

Fig. 12. Variation of Nu/Nu_0 ratio with Re.

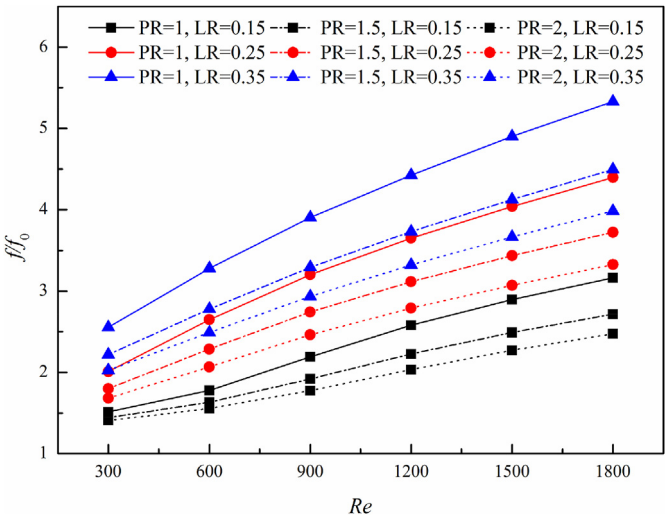

Fig. 13. Variation of f/f_0 ratio with *Re*.

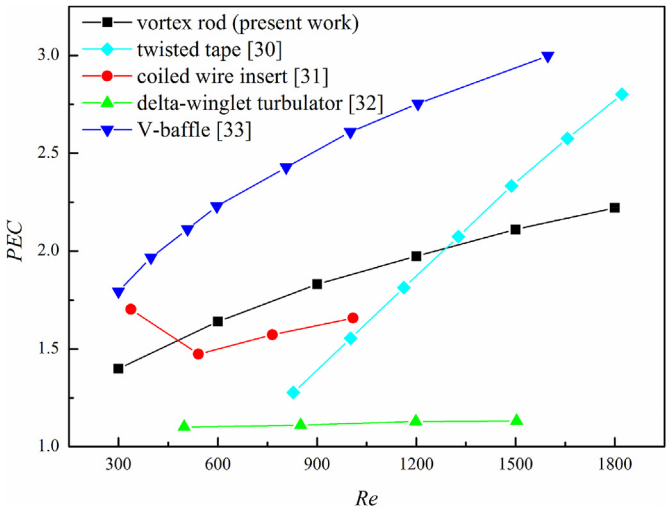

Fig. 15. Comparisons with previous work.

the presence of the vortex rods) and the impingement flows induced by the vortex rods.

4.5. Overall thermo-hydraulic performance evaluation

Fig. 14 displays the evaluation of the overall thermo-hydraulic performance of the water flowing in the tube (inserted with vortex rods) in terms of the performance evaluation criterion (*PEC*). The performance evaluation criterion for the vortex rods tends to increase with increasing *Re* values but decreases with increasing *PR* values. The *PEC* values of all the vortex rod cases are above unity except for the cases with $LR = 0.15$ at $Re = 300$. This indicates that the tube fitted with vortex rods is advantageous compared to a smooth tube for $Re > 300$. In addition, the case of vortex rods at $LR = 0.35$ and $PR = 1$ provides the best overall thermo-hydraulic performance at $Re = 1800$. At $PR = 1$, the maximum *PEC* values of the vortex rods with $LR = 0.15$, 0.25, and 0.35 are, respectively, approximately 1.56, 2.00, and 2.22.

4.6. Comparison with previous work

Fig. 15 shows the comparison of the overall thermo-hydraulic performance between the proposed vortex rod in the present work and previous work. Some widely used turbulators/baffles in practical applications, such as twisted tape [30], coiled wire insert [31], delta-winglet turbulator [32] and V-baffle [33] are selected to perform the comparisons. It is clear from the figure that the vortex rod provides higher thermo-hydraulic performance than the delta-winglet turbulator and coiled wire insert but lower performance than V-baffle. The vortex rod performs better than twisted tape as the Reynolds number is less than 1200. The results indicate that the vortex rod is a promising tube insert for heat transfer enhancement in practical applications. In order to further improve the overall thermo-hydraulic performance of vortex rod, more geometric parameters would be studied in the future work.

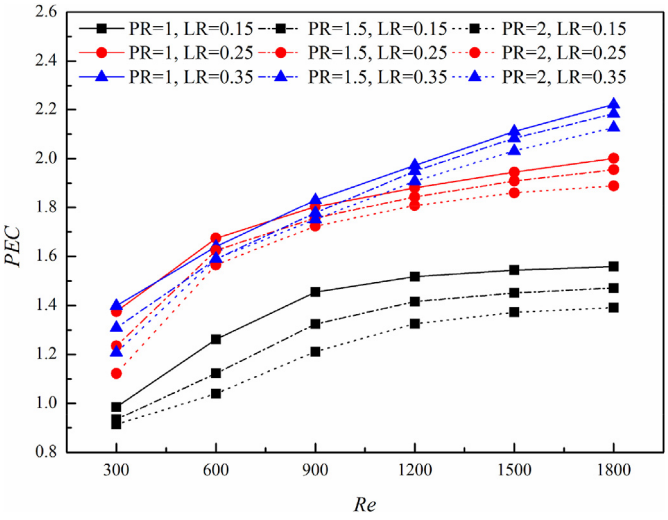

Fig. 14. Variation of *PEC* with *Re*.

5. Conclusions

A numerical analysis was conducted to examine the characteristics of heat transfer and flow friction in a heat exchanger tube fitted with vortex rods at different *LR* and *PR* values under conditions of laminar flow. Details of the flow structures were presented and analyzed. Based on the numerical results, the following main conclusions are deduced:

(1) Vortex rod inserts affect the flow structure in the exchanger tube. The vortex rod inserts with simple geometries generate pairs of counter-rotating vortices or longitudinal swirling flows in the tube. Vortex induced impingement leads to a better fluid mixing between the wall and the core flow regions. Mixing increases the temperature gradient of the thermal boundary layer and causes uniformity in the fluid temperature that enhances heat transfer.

(2) The presence of vortex rods provides a considerable heat transfer augmentation in the tube, leading to a range of values for $Nu/Nu_0 = 1.1–3.9$ with a moderate increase in the pressure drop, and to a range in values for $f/f_0 = 1.4–5.3$. Both the Nu/Nu_0 and the f/f_0 ratio increase with an increase in the *Re* and *LR* values. They also exhibit an increase upon reductions in the *PR* values.

(3) The *PEC* values of all the vortex rod cases are above unity except for the cases with $LR = 0.15$ at $Re = 300$. This indicates that the tube fitted with vortex rods is advantageous over a smooth tube for $Re > 300$. The case of vortex rods at $LR = 0.35$ and $PR = 1$ provides the maximum *PEC* value of approximately 2.22 at $Re = 1800$.

Acknowledgments

The work was supported by the National Key Basic Research Program of China (973 Program) (2013CB228302) and the National Natural Science Foundation of China (51376069).

Nomenclature

b	length of vortex rods, m
C_p	specific heat at constant pressure, J kg^{-1} K^{-1}
CFD	computational fluid dynamics
D	diameter, m
f	friction factor
h	heat transfer coefficient, W m^{-2} K^{-1}
h_{local}	local heat transfer coefficient, W m^{-2} K^{-1}
k	thermal conductivity of fluid, W m^{-1} K^{-1}
L	length of tube, m
LR	relative rod length ratio $= b/D$
Nu	Nusselt number
Nu_{local}	local Nusselt number
p	pitch length of vortex rods, m
P	pressure, Pa
ΔP	pressure drop, Pa
PR	relative rod pitch ratio $= p/D$
PEC	performance evaluation criterion
q	heat flux density, W m^{-2}
R	inner radius of the tube, m
r	radial distance, m
Re	Reynolds number
T	temperature, K
u	flow velocity, m s^{-1}
x_i	space coordinates in Cartesian system, m
x, y, z	Cartesian coordinates
z^*	non-dimensional distance in z-direction

Greek symbols

α	slant angle of vortex rods, °
ρ	fluid density, kg m^{-3}
μ	dynamic viscosity, kg m^{-1} s^{-1}

Subscripts

0	smooth tube
c	center
m	mean
w	wall
i, j	Cartesian coordinates

References

[1] A. Bergles, Recent development in convective heat transfer augmentation, Appl. Mech. Rev. 26 (6) (1973) 675–682.
[2] R.L. Webb, N.-H. Kim, Principle of Enhanced Heat Transfer, Wiley, New York, 1994.
[3] J. Whitham, The effects of retarders in fire tubes of steam boilers, Str. Railw. J. 12 (6) (1896) 374.
[4] S. Saha, U. Gaitonde, A. Date, Heat transfer and pressure drop characteristics of laminar flow in a circular tube fitted with regularly spaced twisted-tape elements, Exp. Therm. Fluid Sci. 2 (3) (1989) 310–322.
[5] Y. Wang, M. Hou, X. Deng, L. Li, C. Huang, H. Huang, G. Zhang, C. Chen, W. Huang, Configuration optimization of regularly spaced short-length twisted tape in a circular tube to enhance turbulent heat transfer using CFD modeling, Appl. Therm. Eng. 31 (6) (2011) 1141–1149.
[6] S. Eiamsa-ard, K. Wongcharee, P. Eiamsa-ard, C. Thianpong, Heat transfer enhancement in a tube using delta-winglet twisted tape inserts, Appl. Therm. Eng. 30 (4) (2010) 310–318.
[7] S. Eiamsa-Ard, P. Promvonge, Performance assessment in a heat exchanger tube with alternate clockwise and counter-clockwise twisted-tape inserts, Int. J. Heat Mass Transf. 53 (7) (2010) 1364–1372.
[8] S. Eiamsa-ard, K. Kiatkittipong, Heat transfer enhancement by multiple twisted tape inserts and TiO_2/water nanofluid, Appl. Therm. Eng. 70 (1) (2014) 896–924.
[9] J. Guo, A. Fan, X. Zhang, W. Liu, A numerical study on heat transfer and friction factor characteristics of laminar flow in a circular tube fitted with center-cleared twisted tape, Int. J. Therm. Sci. 50 (7) (2011) 1263–1270.
[10] X. Zhang, Z. Liu, W. Liu, Numerical studies on heat transfer and flow characteristics for laminar flow in a tube with multiple regularly spaced twisted tapes, Int. J. Therm. Sci. 58 (2012) 157–167.
[11] X. Zhang, Z. Liu, W. Liu, Numerical studies on heat transfer and friction factor characteristics of a tube fitted with helical screw-tape without core-rod inserts, Int. J. Heat Mass Transf. 60 (2013) 490–498.
[12] A. Garcia, P.G. Vicente, A. Viedma, Experimental study of heat transfer enhancement with wire coil inserts in laminar-transition-turbulent regimes at different Prandtl numbers, Int. J. Heat Mass Transf. 48 (21) (2005) 4640–4651.
[13] B.A. Saraç, T. Bali, An experimental study on heat transfer and pressure drop characteristics of decaying swirl flow through a circular pipe with a vortex generator, Exp. Therm. Fluid Sci. 32 (1) (2007) 158–165.
[14] S. Eiamsa-Ard, S. Rattanawong, P. Promvonge, Turbulent convection in round tube equipped with propeller type swirl generators, Int. Commun. Heat Mass Transf. 36 (4) (2009) 357–364.
[15] P. Naphon, Effect of coil-wire insert on heat transfer enhancement and pressure drop of the horizontal concentric tubes, Int. Commun. Heat Mass Transf. 33 (6) (2006) 753–763.
[16] K. Yakut, B. Sahin, Flow-induced vibration analysis of conical rings used for heat transfer enhancement in heat exchangers, Appl. Energy 78 (3) (2004) 273–288.
[17] K. Yakut, B. Sahin, S. Canbazoglu, Performance and flow-induced vibration characteristics for conical-ring turbulators, Appl. Energy 79 (1) (2004) 65–76.
[18] P. Promvonge, S. Eiamsa-ard, Heat transfer behaviors in a tube with combined conical-ring and twisted-tape insert, Int. Commun. Heat Mass Transf. 34 (7) (2007) 849–859.
[19] J. Guo, Y. Yan, W. Liu, F. Jiang, A. Fan, Effects of upwind area of tube inserts on heat transfer and flow resistance characteristics of turbulent flow, Exp. Therm. Fluid Sci. 48 (2013) 147–155.
[20] A. Fan, J. Deng, A. Nakayama, W. Liu, Parametric study on turbulent heat transfer and flow characteristics in a circular tube fitted with louvered strip inserts, Int. J. Heat Mass Transf. 55 (19) (2012) 5205–5213.
[21] S. Caliskan, Experimental investigation of heat transfer in a channel with new winglet-type vortex generators, Int. J. Heat Mass Transf. 78 (2014) 604–614.
[22] P.W. Deshmukh, R.P. Vedula, Heat transfer and friction factor characteristics of turbulent flow through a circular tube fitted with vortex generator inserts, Int. J. Heat Mass Transf. 79 (2014) 551–560.
[23] P. Promvonge, N. Koolnapadol, M. Pimsarn, C. Thianpong, Thermal performance enhancement in a heat exchanger tube fitted with inclined vortex rings, Appl. Therm. Eng. 62 (1) (2014) 285–292.
[24] W. Tu, Y. Tang, B. Zhou, L. Lu, Experimental studies on heat transfer and friction factor characteristics of turbulent flow through a circular tube with small pipe inserts, Int. Commun. Heat Mass Transf. 56 (2014) 1–7.
[25] H. Jia, Z.C. Liu, W. Liu, A. Nakayama, Convective heat transfer optimization based on minimum entransy dissipation in the circular tube, Int. J. Heat Mass Transf. 73 (0) (2014) 124–129.
[26] W. Liu, H. Jia, Z.C. Liu, H.S. Fang, K. Yang, The approach of minimum heat consumption and its applications in convective heat transfer optimization, Int. J. Heat Mass Transf. 57 (1) (2013) 389–396.
[27] H. Jia, W. Liu, Z. Liu, Enhancing convective heat transfer based on minimum power consumption principle, Chem. Eng. Sci. 69 (1) (2012) 225–230.
[28] J. Holman, Heat Transfer, McGraw-Hill, New York, USA, 2002.
[29] R. Webb, Performance evaluation criteria for use of enhanced heat transfer surfaces in heat exchanger design, Int. J. Heat Mass Transf. 24 (4) (1981) 715–726.
[30] K. Wongcharee, S. Eiamsa-Ard, Friction and heat transfer characteristics of laminar swirl flow through the round tubes inserted with alternate clockwise and counter-clockwise twisted-tapes, Int. Commun. Heat Mass Transf. 38 (2011) 348–352.
[31] M. Akhavan-Behabadi, R. Kumar, M. Salimpour, R. Azimi, Pressure drop and heat transfer augmentation due to coiled wire inserts during laminar flow of oil inside a horizontal tube, Int. J. Therm. Sci. 49 (2010) 373–379.
[32] H.E. Ahmed, M. Ahmed, M. Yusoff, Heat transfer enhancement in a triangular duct using compound nanofluids and turbulators, Appl. Therm. Eng. 91 (2015) 191–201.
[33] W. Jedsadaratanachai, N. Jayranaiwachira, P. Promvonge, 3D numerical study on flow structure and heat transfer in a circular tube with V-baffles, Chin. J. Chem. Eng. 23 (2015) 342–349.